

## GaAs lower conduction-band minima: Ordering and properties

D. E. Aspnes

*Bell Laboratories, Murray Hill, New Jersey 07974*

(Received 8 July 1976)

Synchrotron-radiation Schottky-barrier electroreflectance spectra from the Ga  $3d^V$  core levels to the lower  $sp^3$  conduction band have shown that the  $L_6^C$  lower conduction-band minima are located  $170 \pm 30$  meV in energy below the  $X_6^C$  minima in GaAs. Here, we investigate the implications of this ordering, which is opposite to that commonly accepted as correct. We find that, without exception, the results of previous experiments that apparently supported the opposite ordering can be reinterpreted within the  $\Gamma_6^C-L_6^C-X_6^C$  model. By performing a line-shape analysis, we resolve an apparent discrepancy between intraconduction band absorption measurements of the  $X_6^C-\Gamma_6^C$  energy separation. By comparing these optical results with other modulation spectroscopic ( $sp^3$  valence-conduction-band electroreflectance, high-precision reflectance) data, combining these with the results of photoemission, transport (high pressure and high temperature), semiconductor alloy, and luminescence measurements, nonlocal pseudopotential calculations,  $\vec{k}\cdot\vec{p}$  theory, the rigid-valence-band hypothesis, and using the systematics of other tetrahedrally bonded semiconductors with temperature and pressure, we obtain a set of consistent parameters describing the  $\Gamma_6^C$ ,  $L_6^C$ , and  $X_6^C$  lower conduction-band minima of GaAs. This model resolves the former contradictions in the apparent indirect threshold energy as determined previously by photoemission, transport, and optical measurements. Previous photoemission data for cesiated GaAs show clearly after structure reassignment that hot electrons thermalize in the  $L_6^C$  minima. This implies that Gunn oscillator operation in GaAs involves the  $L_6^C$ , and not  $X_6^C$ , conduction-band minima. We obtain the variation of these minima with composition,  $x$ , in the  $\text{GaAs}_{1-x}\text{P}_x$  alloy series, and show that the increase in binding energy of the N isoelectronic trap with increasing As fraction in this series is in qualitative agreement with the prediction of a two-level model wherein a Koster-Slater isoelectronic trap potential interacts with the densities of states of both  $L_6^C$  and  $X_6^C$ . These results have clear implications for the theory of operation of light-emitting diodes of GaAs and its alloys.

### I. INTRODUCTION

The recent observation<sup>1</sup> of  $L_6^C$  conduction-band minima structure at  $170 \pm 30$  meV below that of the  $X_6^C$  minima in Ga  $3d^V$  core-level- $sp^3$ -conduction-band synchrotron-radiation Schottky-barrier electroreflectance (ER) measurements in the 20–22-eV spectral range was surprising. In 1960, Ehrenreich<sup>2</sup> showed that all existing data could be explained within experimental error by assuming that the  $L_6^C$  minima are well above the  $X_6^C$  minima in energy. Since that time, every experiment except core-level ER (Ref. 1) had apparently supported Ehrenreich's now generally accepted hypothesis, although Pitt<sup>3</sup> noted in 1973 several puzzling contradictions in apparent thresholds between (in particular) optical,<sup>4,5</sup> photoemission,<sup>6,7</sup> and transport<sup>8,9</sup> measurements.

Since GaAs is a technologically important material for many reasons, it appeared worthwhile to reinvestigate the results of the other experiments to determine whether the  $\Gamma_6^C-L_6^C-X_6^C$  ordering shown by the core-level ER data might not in fact resolve the contradictions and yield better values for the parameters describing the lower conduction-band structure in GaAs. This would provide a firm basis from which to start new inquiries into the theory of operation of transferred-electron<sup>10</sup> and light-emitting<sup>11</sup> devices using GaAs and

related materials.

We found without exception that these experiments could be reinterpreted to agree with the  $\Gamma_6^C-L_6^C-X_6^C$  ordering of the conduction-band minima. In fact, the apparent threshold contradictions between the optical<sup>4,5</sup> and the photoemission<sup>6,7</sup> data can be resolved in no other way. The parameters obtained for the lower-conduction-band structure of GaAs and of  $\text{GaAs}_{1-x}\text{P}_x$  alloys, and summarized in Tables I and II and Eqs. (16), are consistent not only with the modulation spectroscopic (core-level ER,<sup>1</sup> intraconduction-band absorption,<sup>4,5</sup>  $sp^3$  valence-conduction Schottky-barrier ER,<sup>12</sup> and absorption-edge<sup>13–15</sup>) data, but also with photoemission,<sup>6,7</sup> transport (high pressure<sup>8</sup> and high temperature<sup>9</sup>), and semiconductor alloy<sup>16</sup> and luminescence<sup>16–18</sup> measurements, and also with nonlocal-pseudopotential band-structure calculations,<sup>19,20</sup>  $\vec{k}\cdot\vec{p}$  theory,<sup>21,22</sup> the rigid-band hypothesis,<sup>23</sup> and the systematics of other tetrahedrally bonded semiconductors with temperature<sup>24</sup> and pressure.<sup>25</sup> We show that an apparent discrepancy in the determination of the  $X_6^C-\Gamma_6^C$  energy separation from intraconduction-band absorption measurements<sup>4,5</sup> is due to line-shape interpretation: a proper line-shape analysis not only provides a new and reliable value for this separation, but also demonstrates the square-root nature of the edge singularity of the conduction band in degen-

erately doped  $n$ -type GaAs. Since each experiment measures different quantities, the “best-fit” parameters given in Tables I and II are the result of a number of unique constraints and are therefore quite well determined over a wide range of temperature and pressure.

The optical data are analyzed and discussed in Sec. II. The transport data are treated in Sec. III. Implications of the new ordering are discussed in Sec. IV. We show, for example, that the  $\Gamma_6^C$ - $L_6^C$ - $X_6^C$  ordering provides a natural qualitative explanation of the increase of the measured<sup>18</sup> binding energy of the N isoelectronic trap with increasing As concentration in the GaAs<sub>1-x</sub>P<sub>x</sub> alloy series, and shows that the major features of this trap cannot be explained entirely by assuming a more complex form<sup>26</sup> of the Koster-Slater potential alone,<sup>27</sup> but that any treatment must also consider the contribution of  $L_6^C$ . The combined  $L$ - $X$  nature of the wave function of an electron bound to this trap has clear implications of luminescence efficiency,<sup>11,28</sup> binding energy,<sup>27,29</sup> and other properties of deep centers in GaAs and related materials such as GaAs<sub>1-x</sub>P<sub>x</sub> and Ga<sub>1-x</sub>Al<sub>x</sub>As alloys. The implications for the description of transferred-electron devices<sup>10</sup> and Gunn oscillators,<sup>30</sup> formerly interpreted<sup>10,31,32</sup> exclusively in a  $\Gamma_6^C$ - $X_6^C$  model, are also obvious, although we shall not investigate these in detail at this time.

## II. OPTICAL EXPERIMENTS: THRESHOLD ENERGIES AND TEMPERATURE DEPENDENCES

Optical measurements provide highly accurate data from which to measure threshold energies and their temperature dependences. We discuss parameters determined from these data in this section. The top of the valence band ( $\Gamma_8^V$ ) will be used as the reference energy ( $E=0$ ) throughout.

For simplicity, we shall not follow the self-consistent approach that we used to obtain these lower-conduction-band parameters. Rather, we shall assume initially that all values are correct as given, and discuss according to each experiment those which can be determined most accurately.

### A. $\Gamma_6^C$ absolute minimum

The  $\Gamma_6^C$ - $\Gamma_8^V$  separation has been measured with great accuracy by Sell *et al.*<sup>13,14</sup> and by Panish and Casey.<sup>15</sup> These data were used by Thurmond<sup>33</sup> to determine the coefficients  $\alpha, \beta$  of the Varshni equation,<sup>34</sup>

$$E_{CV} = E_0 - \alpha T^2 / (T + \beta), \quad (1)$$

for this energy gap. Specifically, the expression<sup>33</sup>  $E_{\Gamma} = 1.519$  eV

$$- (5.405 \times 10^{-4} \text{ eV/K}^{-1}) T^2 / (T + 204 \text{ K}) \quad (2)$$

predicts energies that agree with experiment with a mean-square deviation of 2.6 meV. The coefficients are summarized in Table I.

### B. $X_6^C$ relative minima

The  $X_6^C$ - $\Gamma_6^C$  energy separation can be determined directly, in principle, from intraconduction-band absorption measurements in degenerate  $n$ -type material. Balslev<sup>4</sup> and Onton *et al.*<sup>5</sup> reported values of  $0.43 \pm 0.015$  eV at 80 K and  $0.483 \pm 0.015$  eV at 2 K, respectively, for the  $X_6^C$ - $\Gamma_6^C$  separation.<sup>35</sup> The  $\langle 100 \rangle$  symmetry of these higher minima was positively identified by the polarization dependence of the absorption coefficient under uniaxial stress.<sup>4</sup> An indirect determination of the  $X_6^C$ - $\Gamma_6^C$  separation, and an independent verification of the  $\langle 100 \rangle$  symmetry of these minima, was obtained by Craford *et al.*<sup>16</sup> from measurements at 77 K on the lowest (indirect) absorption threshold of GaAs<sub>1-x</sub>P<sub>x</sub> alloys for  $x \geq 0.5$ . An unconstrained extrapolation to  $x=0$  of a best-fit parabola to these data showed that the  $X_6^C$ - $\Gamma_6^C$  separation for GaAs should be about 0.48 eV.

Although the Balslev and Onton *et al.* results apparently differ, their data for similar impurity concentrations are virtually identical: the intraconduction peaks in  $\alpha(E)$  for samples in the  $(1.2-1.5) \times 10^{18}$ -cm<sup>-3</sup> impurity range occur at  $510 \pm 5$  meV in *both* experiments. The data from Onton *et al.*<sup>5</sup> are shown in Fig. 1. The difference in absorption thresholds is therefore simply due to a difference in line-shape interpretations. Balslev<sup>4</sup>

TABLE I. Energies and temperature dependence of  $\Gamma_6^C$ ,  $L_6^C$ , and  $X_6^C$  conduction-band minima of GaAs relative to the top ( $\Gamma_8^V$ ) of the valence band. The Varshni coefficients  $E_0$ ,  $\alpha$ , and  $\beta$  are defined by Eq. (1).

	$E_0$ (eV)	$\alpha$ (eV K <sup>-1</sup> )	$\beta$ (K)
$\Gamma_6^C$	1.519 <sup>a</sup>	$5.405 \times 10^{-4}$ <sup>a</sup>	204 <sup>a</sup>
$L_6^C$	1.815 <sup>b</sup>	$6.05 \times 10^{-4}$ <sup>c</sup>	204 <sup>d</sup>
$X_6^C$	1.981 <sup>e</sup>	$4.6 \times 10^{-4}$ <sup>f</sup>	204 <sup>d</sup>
$X_7^C$	2.383 <sup>g</sup>	$4.6 \times 10^{-4}$ <sup>h</sup>	204 <sup>d</sup>

<sup>a</sup> Reference 33.

<sup>b</sup> From  $X_6^C$  and core-level Schottky-barrier electroreflectance (Ref. 1).

<sup>c</sup> Optical and high-temperature transport; see text.

<sup>d</sup> Postulated to equal  $\Gamma_6^C$  value; see text.

<sup>e</sup> Intraconduction absorption (Ref. 5) and line-shape analysis.

<sup>f</sup> By analogy to GaP (Ref. 41), supported by rigid-band model (Ref. 23).

<sup>g</sup> From  $X_6^C$  and Schottky-barrier electroreflectance (Ref. 12).

<sup>h</sup> Postulated to equal  $X_6^C$  value.

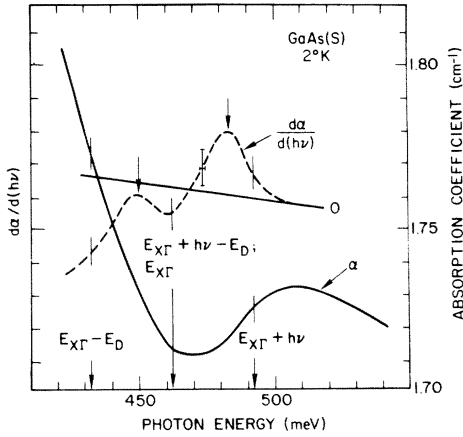


FIG. 1. Absorption coefficient (—) and its first energy derivative (---) of degenerate  $n$ -type GaAs at 2 K in the energy range of intraconduction-band absorption from  $\Gamma_6^C$  to  $X_6^C$  (after Ref. 5). Our threshold energy  $E_{X\Gamma}$  is obtained by analysis of these line shapes as described in the text.  $E_D$  and  $h\nu$  are the degeneracy energy of the conduction band and the energy of the emitted phonon, respectively, which are coincidentally equal for this particular sample.

chose the energy at the onset of excess (intraband) absorption as that corresponding to the  $X_6^C - \Gamma_6^C$  separation,  $E_{X\Gamma}$ , plus that,  $h\nu$ , of an emitted phonon. Onton *et al.*<sup>5</sup> resolved this edge into separate zero-phonon and phonon-emission structures by wavelength-modulated transmission measurements, as seen in Fig. 1, and assigned the peak of the phonon-emission structure at 0.483 eV in  $d\alpha(E)/dE$ , as indicated by the arrow, to the energy corresponding to  $E_{X\Gamma} + h\nu - E_D$ , where  $E_D$  is the degeneracy level of the  $\Gamma_6^C$  minimum.

The latter interpretation assumes in effect that the singularity in  $d\alpha(E)/dE$  occurs between the Fermi level of the electrons in  $\Gamma_6^C$  and the lowest (empty) states of  $X_6^C$ . Since intraconduction-band absorption in the constant matrix element approximation is expressed as a convolution of occupied and unoccupied densities of states, it is not clear that the assignment<sup>5</sup> of  $(E_{X\Gamma} + h\nu - E_D)$  to the peak in  $d\alpha(E)/dE$  is correct for finite  $E_D$ , although it is certainly true in the limit that  $E_D \rightarrow 0$ . To investigate this point further, we calculated line shapes  $d\alpha/dE$  from several simple parabolic model densities of states according to the standard expression<sup>36</sup>

$$\alpha(E) \propto \int_0^{K_d} k_\Gamma^n dk_\Gamma \int_0^\infty k_X^2 dk_X \times \delta(\hbar\omega - E_{X\Gamma} - h\nu + k_\Gamma^2 - k_X^2). \quad (3)$$

In Eq. (3),  $k_\Gamma$  and  $k_X$  are the radial wave-vector components measured from the  $\Gamma_6^C$  and  $X_6^C$  critical

points, respectively,  $K_d^2 = E_D$  is the degeneracy level of the  $\Gamma_6^C$  minimum, and  $\hbar\omega$  is the photon energy. The effective masses do not affect the line shape and have been scaled out by a coordinate transformation on  $k$ . The expression was evaluated and energy differentiated in closed form for three  $\Gamma_6^C$  densities of states:  $n=1$  [ $2D M_0$  (two-dimensional  $M_0$ ) or step threshold],  $n=2$  ( $3D M_0$  or square-root threshold), and  $n=3$  (" $4D M_0$ " or energy-linear threshold). In effect,  $n$  determines the energy distribution of electrons from 0 to  $E_D$  from which the intraband absorption process originates.

The results of the calculations are shown in Fig. 2. All curves, for both  $\alpha$  and  $d\alpha/dE$ , have been normalized to yield a peak value of 1 in  $d\alpha/dE$ . Although the different model densities of states affect  $\alpha(E)$  only weakly, it is obvious that  $d\alpha/dE$  is very sensitive to the details of the energy distribution of the conduction electrons at  $\Gamma_6^C$ . In particular, the peaks of  $d\alpha(E)/dE$  occur at different energies relative to  $E_{X\Gamma}$ ,  $E_D$ , and  $h\nu$ , depending upon the model assumed. But in no case does the peak correspond to  $E_{X\Gamma} + h\nu - E_D$ , as was assumed in Ref. 5.

The  $3D M_0$  exponent,  $n=2$ , gives the best qualitative agreement to the line shape  $d\alpha(E)/dE$  shown in Fig. 1, obtained for a sample<sup>5</sup> with  $n_c = 1.2 \times 10^{18} \text{ cm}^{-3}$ . The  $n=2$  exponent is also expected from physical arguments, since at these carrier concentrations the electron-hole Coulomb interaction is completely screened.<sup>37</sup> Therefore, we conclude that the peak in  $d\alpha(E)/dE$  at 0.483 eV occurs by Fig. 2 at  $(\Delta E_{X\Gamma} + h\nu - 0.3E_D)$ . Since  $h\nu = 30 \pm 1 \text{ meV}$ ,<sup>5,38</sup> and  $E_D = 30 \text{ meV}$ ,<sup>5,39</sup> for  $n_c = 1.2 \times 10^{18}$

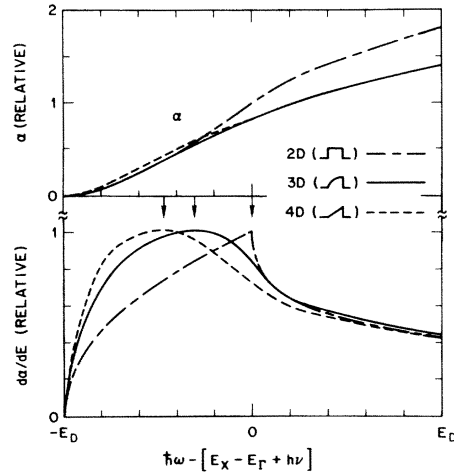


FIG. 2. Calculated absorption coefficient  $\alpha$  and its energy derivative  $d\alpha/dE$  from Eq. (3) for several model densities of states as indicated. Arrows indicate peak values in  $d\alpha/dE$ .

$\text{cm}^{-3}$ , we find  $E_{X\Gamma} = 0.462 \pm 0.005$  eV at 2 K. This energy is in excellent agreement with that for the onset of phonon-assisted intraband absorption, indicated by the arrow in Fig. 1, as predicted by the theoretical  $n=2$  line shape of Fig. 2. It also agrees well with the value obtained in Ref. 4 if it is assumed (in agreement with Ref. 5) that intraconduction-band absorption is initiated by a zero-phonon process, in which case a phonon energy is *not* to be subtracted from the apparent threshold. Thus a proper line-shape interpretation resolves all discrepancies between the apparently different  $E_{X\Gamma}$  values obtained by intraconduction-band absorption.

The  $X_6^C - \Gamma_8^V$  separation of  $1.981 \pm 0.006$  eV at 2 K follows directly from the preceding results. The temperature dependence of this separation cannot be measured directly, but can be obtained as follows. The coefficient  $\beta$  in the Varshni equation has been shown to be related to the Debye temperature for the fundamental absorption edges of Si, Ge, GaP, and GaAs.<sup>40</sup> Since the fundamental absorption edges in Si and GaP are indirect to conduction-band minima along  $\langle 100 \rangle$  and at  $X_6^C$ , respectively, it is clear that a similar relation should hold in GaAs. Thus we postulate  $\beta = 204$  K for the  $X_6^C - \Gamma_8^V$  separation, and similarly, also for the  $L_6^C - \Gamma_8^V$  separation on the basis of the same results for Ge.<sup>40</sup> The coefficient  $\alpha$  in Eq. (2) is more difficult to obtain. We note, however, that the average variation of the  $X_6^C - \Gamma_8^V$  gap in the 110–300-K range in GaP is about 80% that of the  $\Gamma_6^C - \Gamma_8^V$  gap.<sup>41</sup> Further, the rigid-band postulate of Auvergne *et al.*<sup>23</sup> when combined with the average temperature shift of the  $E_0(\Gamma_6^C - \Gamma_8^V)$  gap from 77 to 295 K ( $-3.9 \times 10^{-4}$  eV  $\text{K}^{-1}$ )<sup>33</sup> and that of the  $E_2(X_6^V - X_6^C)$  transition ( $-3.3 \times 10^{-4}$  eV  $\text{K}^{-1}$ )<sup>42</sup> shows an  $X_6^C - \Gamma_8^V$  variation approximately (80–90)% that of  $\Gamma_6^C - \Gamma_8^V$ . Accordingly, we take the  $X_6^C - \Gamma_8^V$  coefficient  $\alpha$  to be 0.85 that of the corresponding  $\Gamma_6^C - \Gamma_8^V$  coefficient, but the exact value should be regarded as uncertain. Nevertheless, analysis of high-pressure Hall effect and resistivity data,<sup>8</sup> to be discussed in Sec. III, supports these values of  $\alpha$  and  $\beta$  to within experimental uncertainty.

### C. $L_6^C$ relative minima

The  $X_6^C - L_6^C$  energy separation has been determined from core-level ER measurements<sup>1</sup> to be  $0.17 \pm 0.03$  eV at 110 K, from the location of the “anomalous” structure in the spectrum shown in Fig. 3. To find the  $L_6^C - \Gamma_8^V$  separation at 0 K, the coefficient  $\alpha$  for the  $L_6^C - \Gamma_8^V$  separation must be determined. Following the Auvergne *et al.* postulate of rigid valence bands<sup>23</sup> and our measured energy shift of 115 meV of the  $E_1(L_6^C - L_6^V)$  transition from 4 to 295 K from Schottky-barrier

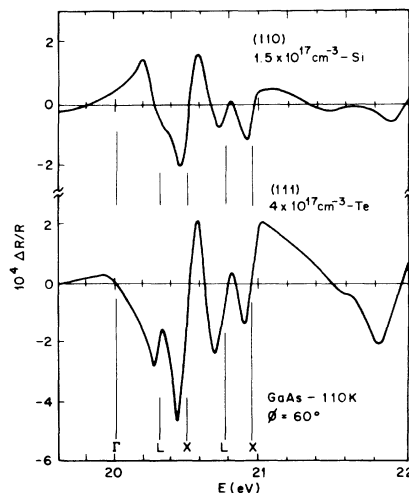


FIG. 3. Core-level Schottky-barrier electroreflectance spectra of lightly (top) and heavily doped (bottom) GaAs crystals at 110 K (after Ref. 1). Spectral features due to critical points between the Ga  $3d^V$  core levels and the  $\Gamma_6^C$ ,  $L_6^C$ , and  $X_6^C$  local conduction-band minima are indicated.

electroreflectance measurements in the 3-eV range,<sup>12</sup> we calculate  $\alpha \cong 6.5 \times 10^{-4}$  eV  $\text{K}^{-1}$  for the  $L_6^C - \Gamma_8^V$  separation. But high-temperature transport measurements,<sup>9</sup> to be discussed in Sec. III, indicate that this value is too high. We have chosen  $6.05 \times 10^{-4}$  eV  $\text{K}^{-1}$  as a compromise value between the two types of experiments, but again it should be regarded as fairly uncertain. With  $\alpha$  and  $E_{XL}$  at 110 K, the  $L_6^C - \Gamma_8^V$  energy separation at 0 K shown in Table I follows directly.

### D. $X_7^C$ relative minima

The  $X_7^C$  minima do not produce observable structure in Fig. 3 because of matrix element effects. Balslev<sup>4</sup> first determined the  $X_7^C - X_6^C$  energy separation as  $0.35 \pm 0.05$  eV at 80 K from structure in intraconduction-band absorption spectra. Later Schottky-barrier ER measurements<sup>12</sup> gave  $0.402 \pm 0.010$  eV at 10 K for this quantity. We assume that the Varshni  $\alpha$  and  $\beta$  coefficients for the  $X_7^C - \Gamma_8^V$  separation are the same as those for the  $X_6^C - \Gamma_8^V$  separation, although no confirming measurements are available. At present, this is not essential since the  $X_7^C$  minima apparently do lie sufficiently far above the  $X_6^C$  minima so as not to affect transport properties.

## III. OTHER EXPERIMENTS

In this section, we investigate other classes of experiments to determine whether their results, previously interpreted as supporting the  $\Gamma$ - $X$  model, cannot also be explained by means of the

$\Gamma$ - $L$ - $X$  model obtained from the modulation spectroscopic data as discussed in Sec. II. We find not only that these results can be reinterpreted, but also that photoemission data gives unambiguous further evidence for the validity of the  $\Gamma$ - $L$ - $X$  model. The transport experiments provide limits on the allowed ranges of certain parameters of these conduction-band minima.

#### A. Photoemission

Photoemission experiments providing information about lower-lying conduction-band minima in GaAs have been performed by James *et al.*<sup>6</sup> and James and Moll.<sup>7</sup> The energy distribution curves (EDC) obtained at 300 K in the least heavily doped ( $1 \times 10^{19} \text{ cm}^{-3} \text{ Zn}$ ) sample from the latter work are shown in Fig. 4. Positions of the optically determined minima, calculated at 300 K from the data of Table I, are also indicated.

The peak in the EDC at 1.43 eV, due to photoelectrons thermalized at  $\Gamma_6^C$ , agrees well with the optical value of 1.423 eV from Table I. The data in Table I place the  $L_6^C$  and  $X_6^C$  minima at 300 K at 1.707 and 1.899 eV, respectively. The EDC peak at 1.75 eV is therefore unquestionably below the  $X_6^C$  threshold and can arise only from electrons thermalized at  $L_6^C$ . It is not possible to explain the presence of this peak within the  $\Gamma$ - $X$  model, in view of the intraconduction absorption results discussed in Sec. II.

James and Moll<sup>7</sup> have discussed the energy separation between the  $\Gamma_6^C$  and " $X_6^C$ " peaks in the EDC in terms of experimental uncertainties and the threshold function for photoemission. They note that the apparent 0.35-eV separation at 300 K in their best data is greater than the actual separation,

which may be as low as 0.28 eV but has a probable best value of 0.33 eV. The optical  $L_6^C$ - $\Gamma_6^C$  separation from Table I has a probable best value of  $0.28 \pm 0.05$  eV at 300 K, and thus overlaps with the photoemission results. Further proof of the validity of the reassignment of the photoemission  $X_6^C$  peak to  $L_6^C$  follows from the James *et al.* observation that the best value of the  $X_6^C$ - $\Gamma_6^C$  peak separation *increases* by 0.03 eV upon cooling from 300 to 80 K. From Table I, the  $L_6^C$ - $\Gamma_6^C$  separation increases by 0.010 eV over this range while the  $X_6^C$ - $\Gamma_6^C$  separation *decreases* by 0.013 eV. A more rapid temperature variation of the  $E_1(L_6^C-L_6^V)$  transition energy relative to that of  $E_0(\Gamma_6^C-\Gamma_8^V)$  is a well-known property of tetrahedrally bonded semiconductors.<sup>23</sup> Thus the rigid-band hypothesis<sup>23</sup> together with the assignment of the 1.75-eV peak to  $L_6^C$  provides a natural explanation of this otherwise puzzling temperature dependence of the energy separation measured by photoemission.

No obvious structure appears in the EDC data near 1.9 eV, the predicted threshold of the  $X_6^C$  minima. This is not surprising, since the  $X_7^C$  structure is likewise not clearly evident from these spectra. Although it is tempting to assign the 2.3-eV structure to  $X_7^C$ , the variation of its apparent energy with photon energy suggests that these structures are due in part to final-state effects. We note that these results provide direct evidence that hot electrons in the conduction band thermalize to  $L_6^C$  and not  $X_6^C$ , and that Gunn-oscillator operation in GaAs involves the  $L_6^C$ , not  $X_6^C$ , minima.

#### B. High-temperature Hall effect; mobilities and densities of states of GaAs conduction-band minima

The most careful high-temperature Hall-effect measurements on GaAs have been done by Blood,<sup>9</sup> using high-purity epitaxial samples where the substrate material was etched away. The measurements were performed between 600 and 700 K, where substantial [(10–20)%] electron transfer to the higher conduction-band minima occurs. The results, expressed in terms of the Hall coefficient  $R_H$  as

$$[R_H(T) - R_H(500 \text{ K})] / R_H(500 \text{ K}), \quad (4)$$

are shown in Fig. 5. The measured slope of this curve,  $0.38 \pm 0.05$  eV, is interpreted<sup>9</sup> as the activation ( $X_6^C$ - $\Gamma_6^C$  separation) energy in the Ehrenreich  $\Gamma$ - $X$  model.

To investigate the  $\Gamma$ - $L$ - $X$  interpretation of these data, we use the Hall coefficient expression for multiple minima<sup>43,44</sup>

$$R_H = \frac{n_\Gamma \mu_\Gamma^2 + n_L \mu_L^2 + n_X \mu_X^2}{e(n_\Gamma \mu_\Gamma + n_L \mu_L + n_X \mu_X)^2}, \quad (5)$$

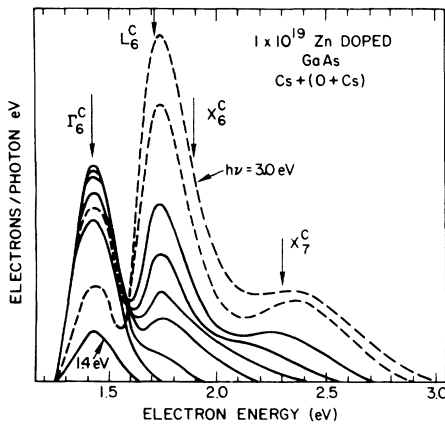


FIG. 4. Energy distribution curves obtained at 300 K from heavily doped  $p$ -type GaAs (after Ref. 7). The energies of the  $\Gamma_6^C$ ,  $L_6^C$ ,  $X_6^C$ , and  $X_7^C$  thresholds calculated from the data in Table I are indicated.

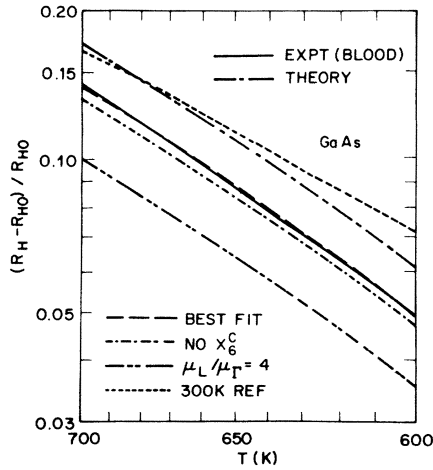


FIG. 5. Activation energy plot of high-temperature transport data (after Ref. 9) and from various calculations within the  $\Gamma$ - $L$ - $X$  model (see text).

where  $n_\Gamma$ ,  $n_L$ , and  $n_X$  are the electron concentrations and  $\mu_\Gamma$ ,  $\mu_L$ , and  $\mu_X$  are the mobilities of the respective minima.

To evaluate Eq. (4) within the three-level model, the various quantities and their temperature dependences must be estimated. We consider first the carrier concentrations  $n_\Gamma$ ,  $n_L$ , and  $n_X$ , which

have the most rapid temperature dependences and provide the main contribution to the apparent activation energy.

For sufficiently low carrier concentrations such that Boltzmann statistics apply,

$$n_\zeta = N_{D\zeta} e^{-(E_\zeta - E_F)/kT}, \quad (6)$$

where  $\zeta = \Gamma, L, \text{ or } X$ ;  $E_\zeta$  and  $N_{D\zeta}$  are the threshold energy and density of states of the  $\zeta$  minimum, and  $E_F$  is the Fermi level. The relative occupation is determined from the above parameters and the charge neutrality equation

$$n_\Gamma + n_L + n_X = N_D, \quad (7)$$

where  $N_D$  is the donor concentration. The threshold energies as a function of temperature are given by Eq. (2) and the data of Table I.

The density of states has the general form<sup>36</sup>

$$N_{D\zeta} = \frac{1}{4} (2 m_\zeta^* kT / \pi \hbar^2)^{3/2} \quad (8)$$

for a simple parabolic band, where the density-of-states mass,

$$(m_\zeta^*)^{3/2} = N m_{t\zeta} m_{l\zeta}^{1/2}, \quad (9)$$

includes both the number of equivalent minima,  $N$ , and the transverse and longitudinal masses,  $m_{t\zeta}$  and  $m_{l\zeta}$ , of the local minima.

The isotropic  $\Gamma_6^C$  mass at 2 K is  $m_{t\Gamma} = m_{l\Gamma}$

TABLE II. Summary of various parameters describing the  $\Gamma_6^C$ ,  $L_6^C$ , and  $X_6^C$  lower conduction-band minima of GaAs.

Quantity	$\Gamma_6^C$	$L_6^C$	$X_6^C$
$N$	1	4	3
$m_l$	$0.067m_e^a$	$1.9m_e^b$	...
$m_t$	...	$0.0754m_e^c$	...
$m^*(0\text{ K})$	$0.067m_e^d$	$0.56m_e^d$	$0.85m_e^e$
$E_P$	$7.51\text{ eV}^f$	$19.3\text{ eV}$	...
$\Delta$	$0.341\text{ eV}^g$	...	...
$m^*(295\text{ K})$	$0.063m_e$	$0.55m_e$	$0.85m_e$
$m^*(650\text{ K})$	$0.056m_e$	$0.52m_e$	$0.85m_e$
$\mu$	$7350\text{ cm}^2\text{V}^{-1}\text{sec}^{-1}\text{h}$	$920\text{ cm}^2\text{V}^{-1}\text{sec}^{-1}\text{i}$	$300\text{ cm}^2\text{V}^{-1}\text{sec}^{-1}\text{i}$
$a(295\text{ K})$	$1.425\text{ eV}^j$	$1.710\text{ eV}^j$	$1.901\text{ eV}^j$
$b(295\text{ K})$	$0.0126\text{ eV/kbar}^k$	$0.0055\text{ eV/kbar}^l$	$-0.0015\text{ eV/kbar}^l$
$c(295\text{ K})$	$-3.77 \times 10^{-5}\text{ eV/kbar}^2\text{k}$	$-3.77 \times 10^{-5}\text{ eV/kbar}^2\text{m}$	$-3.77 \times 10^{-5}\text{ eV/kbar}^2\text{m}$

<sup>a</sup> Reference 45.

<sup>b</sup> Estimated value, see text.

<sup>c</sup>  $\bar{k} \cdot \bar{p}$  theory and Schottky-barrier electroreflectance (Ref. 12).

<sup>d</sup> Calculated from Eq. (9).

<sup>e</sup> Value from Ref. 8.

<sup>f</sup> Calculated as described in text.

<sup>g</sup> Reference 12.

<sup>h</sup> Reference 8.

<sup>i</sup> Best-fit value to high-temperature and high-pressure transport data.

<sup>j</sup> From Table I.

<sup>k</sup> Reference 58.

<sup>l</sup> Best-fit value; see also Ref. 25.

<sup>m</sup> Assumed equal to  $\Gamma_6^C$  value.

$= 0.067m_e$ .<sup>45</sup> The variation of this mass with temperature and/or pressure can be calculated from  $\vec{k} \cdot \vec{p}$  theory according to<sup>21</sup>

$$\frac{m_e}{m_{\Gamma}^*} = 1 + E_{P\Gamma} \left( \frac{2}{E_{\Gamma}} + \frac{1}{E_{\Gamma} + \Delta_0} \right), \quad (10)$$

where  $E_{P\Gamma}$  is an energy related to the momentum matrix element, and  $\Delta_0 = 0.341$  eV is the spin-orbit splitting,<sup>12</sup>  $\Gamma_8^V - \Gamma_7^V$ . From these data and Table I, we calculate  $E_{P\Gamma} = 7.51$  eV as shown in Table II. Values of  $m_{\Gamma}^*$  for any  $E_{\Gamma}$  can be calculated from Eq. (10); those at 295 and 650 K for use with the high-pressure and high-temperature data are also listed in Table II.

The masses at  $L_6^C$  have not been measured directly, although the transverse mass can be inferred from Schottky-barrier electroreflectance measurements of the transverse interband reduced mass at  $L$ ,  $\mu_{iL} = 0.055m_e$ ,<sup>12</sup> together with the  $\vec{k} \cdot \vec{p}$  expressions<sup>22</sup>

$$\frac{m_e}{\mu_{iL}} = E_{PL} \left( \frac{2}{E_1 + \Delta_1} + \frac{1}{E_1} \right), \quad (11a)$$

$$\frac{m_e}{m_{iL}^*} = 1 + E_{PL} \left( \frac{1}{E_1} + \frac{1}{E_1 + \Delta_1} \right). \quad (11b)$$

Here, the interband energy separations  $E_1 = L_6^C - L_6^V = 3.041$  eV and  $\Delta_1 = L_6^V - L_{4,5}^V = 0.220$  eV are given by low-temperature Schottky-barrier electroreflectance measurements.<sup>12</sup> From these data, we calculate the values shown in Table II.

The longitudinal mass at  $L_6^C$  has not been determined. Band-structure calculations for Ge show  $m_{iL} = 1.57m_e$ .<sup>46</sup> This value should be somewhat smaller than that for GaAs, since the  $\Gamma_8^V - \Gamma_6^V$  separation is slightly less in GaAs (1.23 instead of 1.51 eV) and therefore the conduction bands, which closely parallel the valence bands near  $L$ , are slightly flatter. Scaling the Ge mass upwards by the energy difference ratio leads to a longitudinal mass value of  $1.9m_e$ , which is similar to that ( $1.7m_e$ ) observed at  $X_6^C$  in GaP.<sup>47</sup> The value  $m_{iL} = 1.9m_e$  leads to a density-of-states mass of  $m_{L_6^C}^* = 0.56m_e$  at 0 K, as given in Table II.

For  $X_6^C$ , a density-of-states mass of  $0.85m_e$  was calculated by Pitt and Lees<sup>8</sup> from their high-pressure Hall-effect and resistivity data. Although this is derived on the basis of the  $\Gamma$ - $X$  model and depends also on the value assumed for the conduction-band mass at  $\Gamma_6^C$ , this value is nevertheless in good agreement with that,  $m_{X_6^C}^* = 0.82m_e$ , determined by Onton for GaP.<sup>47</sup> We shall assume here that  $m_{X_6^C}^* = 0.85m_e$  in agreement with Pitt and Lees.<sup>8</sup>

The temperature dependence of the density-of-states masses for  $\Gamma_6^C$  and  $L_6^C$  arises from the temperature dependence of the energy gaps, which affects  $m_i$ . Using the data of Table I and  $\vec{k} \cdot \vec{p}$

theory, the values of  $m^*$  at 295 and 650 K, for use in the analysis of high-pressure and high-temperature transport data, are calculated as shown in Table II. No temperature dependence is assumed for the mass at  $X_6^C$ , in view of the large energy ( $\sim 5$  eV)<sup>12</sup> of the  $E_2$  transition in GaAs. Also, the small variation in  $m^*$  for  $\Gamma_6^C$  and  $L_6^C$  over the 600–700-K temperature range will be neglected.

The densities of states for  $\Gamma_6^C$ ,  $L_6^C$ , and  $X_6^C$  could be calculated directly from the data of Table II using the simple parabolic form, Eq. (8). But Hilsum<sup>48</sup> has suggested that  $\Gamma_6^C$  nonparabolicity should make the activation energy in high-temperature Hall measurements appear larger than the true value, because the excess density of states near  $\Gamma_6^C$  due to nonparabolicity competes with the indirect minima for the high-temperature tail of the electron distribution. In order to investigate this, we have incorporated nonparabolicity into the density of states,  $N_{D\Gamma}$ , for  $\Gamma_6^C$  by evaluating the density-of-states integral numerically, using the expression

$$a_B^3 N_D^{\Gamma} = (7.142 \times 10^{-4}) (m_{\Gamma}^*/m_e)^{3/2} (\Delta E/eV)^{3/2} \times \int_0^{\infty} z^2 dz e^{-\Delta E[(1+z^2)^{1/2}-1]/kT}, \quad (12a)$$

where  $a_B$  is the Bohr radius and  $\Delta E$  is a nonparabolicity parameter where

$$E_{\Gamma}(k_{\Gamma}) = E_{\Gamma}(0) + \Delta E \left[ (1 + \hbar^2 k_{\Gamma}^2 / m_{\Gamma}^* \Delta E)^{1/2} - 1 \right] \quad (12b)$$

$$\cong E_{\Gamma}(0) + \frac{\hbar^2 k_{\Gamma}^2}{2m_{\Gamma}^*} - \frac{\hbar^4 k_{\Gamma}^4}{8m_{\Gamma}^{*2} \Delta E} + \dots \quad (12c)$$

This expression is essentially the conduction-band energy in the  $\vec{k} \cdot \vec{p}$  two-band model, but modified so that the energy variation changes from quadratic to linear at a wave vector  $K_0$ . In units of  $K_{\Gamma X}$ , the Brillouin-zone length from  $\Gamma_6^C$  to  $X_6^C$ ,

$$K_0/K_{\Gamma X} \cong 1/(140\Delta E/eV)^{1/2}, \quad (12d)$$

using parameters for GaAs. Equations (12) reduce to the usual parabolic-band result in the limit of large  $\Delta E$ . For GaAs, band-structure calculations<sup>19,20</sup> suggest that  $K_0/K_{\Gamma X} \cong 0.05$ , in which case  $\Delta E \cong 0.35$  eV. We shall use this value to include nonparabolicity for the density of states around  $\Gamma_6^C$ . Thus the terms  $n_{\Gamma}$ ,  $n_L$ , and  $n_X$  in Eq. (5) are determined.

In order to estimate the mobilities in Eq. (5) to investigate the high-temperature transport data, it is necessary to find their values (or more precisely their ratios) in the 600–700-K temperature range. The mobility of carriers in the  $\Gamma_6^C$

and  $X_6^C$  minima at room temperature has been discussed by Pitt and Lees.<sup>8</sup> Polar-optical scattering predominates in the  $\Gamma_6^C$  conduction-band minimum,<sup>49,50</sup> leading to a mass dependence  $\mu \sim m^{*-3/2}$  and an observed<sup>9</sup> temperature dependence of the order of  $\mu \sim T^{-1.25}$  over a 300–500-K temperature range, in good agreement with theory.<sup>9,50</sup> At  $L_6^C$  and  $X_6^C$ , intravalley scattering is an additional mechanism which has been estimated to dominate the mobility in the  $X_6^C$  minima.<sup>51,52</sup> Intravalley scattering leads to a larger negative temperature coefficient,<sup>53</sup> although in GaP the observed<sup>54</sup> value of  $-1.7$  is not significantly different from that of  $\Gamma_6^C$ . Presumably, similar results should obtain for the temperature dependence of the mobility at  $L_6^C$  as well as  $X_6^C$  in GaAs. We therefore assume that the mobility ratios at  $\Gamma_6^C$ ,  $L_6^C$ , and  $X_6^C$  are essentially independent of temperature, and thus keep their room-temperature ratios in the 600–700-K range. The assumption for  $X_6^C$  is almost irrelevant since only a negligible fraction ( $<1\%$ ) of carriers is transferred to these minima, even at 700 K.

The room-temperature conductivity mobility at  $\Gamma_6^C$  of high-purity GaAs is of the order of  $7000\text{--}8000\text{ cm}^2\text{ V}^{-1}\text{ sec}^{-1}$ .<sup>8,55</sup> Pitt and Lees<sup>8</sup> quote a Hall mobility of  $\mu_H = 7350\text{ cm}^2\text{ V}^{-1}\text{ sec}^{-1}$  for the high-quality crystal G62A, the data from which we analyze here. The mobility at  $X_6^C$  at 50 kbar was found to be  $\mu_H(50\text{ kbar}) = 330\text{ cm}^2\text{ V}^{-1}\text{ sec}^{-1}$  and was extrapolated to  $375\text{ cm}^2\text{ V}^{-1}\text{ sec}^{-1}$  at atmospheric pressure. The mobility of carriers in the  $L_6^C$  minima cannot be inferred from values for Ge, since inversion symmetry is absent in GaAs, but measurements of the  $\Gamma_6^C/L_6^C$  mobility ratio for GaSb in hydrostatic pressure experiments show that it is of the order of 7.5.<sup>56,57</sup> The GaSb results show further that the  $\Gamma_6^C/X_6^C$  mobility ratio is approximately 32, in fair agreement with the value 20 calculated from the Pitt-Lees measurements.<sup>8</sup> Mobilities at  $X_6^C$  show a considerable sample-dependent variation that cannot always be correlated to those at  $\Gamma_6^C$  (Ref. 8); this is presumably also true for carriers in the  $L_6^C$  minima, so exact values cannot be assigned.

In view of the above, it is apparent that upper limits on the mobility at  $X_6^C$  and  $L_6^C$  should be about  $400\text{ cm}^2\text{ V}^{-1}\text{ sec}^{-1}$  and  $1000\text{ cm}^2\text{ V}^{-1}\text{ sec}^{-1}$ , respectively, at room temperature. The values for  $\mu_L$  and  $\mu_X$  shown in Table II, which differ only slightly from the above estimates, were those that gave the best fit to both high-temperature and high-pressure transport data.

From these considerations, Eq. (5) was evaluated numerically for a number of combinations of parameters. Those having the greatest effect were the  $\Gamma_6^C-L_6^C$  separation energy at 650 K, the

$\mu_L/\mu_\Gamma$  mobility ratio, the conduction-band nonparabolicity, and the reference temperature. The  $L_6^C-\Gamma_6^C$  separation energy at 0 K and the Varshni parameter  $\alpha_L$  could be mutually adjusted to hold a fixed  $L_6^C-\Gamma_6^C$  separation at 650 K, but this had only a minor influence on the slope.

The influence of various modifications is shown in Fig. 5. Surprisingly, none of the adjustments except varying the reference temperature modified the apparent slope by more than  $\pm 0.02$  eV from the best-fit value 0.38 eV, even though the  $L_6^C-\Gamma_6^C$  separation energy near 650 K is almost 0.1 eV less. This was due to partial filling (3%) of the  $L_6^C$  minima at the experimental reference temperature of 500 K: a recalculation using a reference temperature of 300 K (0.02% filling) produced a slope of 0.30 eV, in good agreement with the actual "best-fit"  $L_6^C-\Gamma_6^C$  energy separation of 0.28 eV near 650 K. The remaining discrepancy is due to the influence of the  $X_6^C$  minima at slightly higher energy. The remaining adjustments merely served to move the calculated curves up or down in direct proportion to the way the modification affected the influence of the  $L_6^C$  minima relative to the  $\Gamma_6^C$  region. Thus halving the mobility ratio  $\mu_L/\mu_\Gamma$ , as seen in Fig. 5, effectively lessens the importance of  $L_6^C$  (the minima become more similar) and the Hall ratio becomes smaller. Similarly, increasing the relative importance of  $L_6^C$  by decreasing the nonparabolicity of  $\Gamma_6^C$  or reducing the  $L_6^C-\Gamma_6^C$  separation causes the Hall ratio to increase. We note that the nonparabolicity of  $\Gamma_6^C$  had very little influence on the slope of the theoretical curves. Eliminating the influence of the  $X_6^C$  minima entirely is also seen to have very little effect.

The "best fit" solution of Fig. 5, defined in terms of overall consistency with respect to all experiments considered here, differs from that given by the parameters of Tables I and II and labeled "Theory" in Fig. 5, in that the  $L_6^C-\Gamma_6^C$  energy separation is 15 meV more at 650 K than the value 0.264 eV calculated from Table I. The difference amounts to a change of 15 meV in the  $L_6^C$  energy at 0 K, or a change of  $0.3 \times 10^{-4}\text{ eV K}^{-1}$  in the Varshni coefficient  $\alpha_L$ . We have chosen the  $L_6^C$  energy at 0 K in Table I with greater emphasis on the optical and transport data below 300 K, and have chosen  $\alpha_L$  as a compromise between the somewhat larger value suggested by the optical data and the results of the high-temperature transport experiment.<sup>9</sup> The differences are minor and within experimental uncertainty.

It is clear that the high-temperature transport data are compatible with the  $\Gamma_6^C-L_6^C-X_6^C$  model proposed here. These data provide useful information on the  $L_6^C-\Gamma_6^C$  separation at elevated temperatures, as well as suggesting limits on the



mobility ratio  $\mu_L/\mu_\Gamma$ . The  $X_6^C$  minima have only a minor influence on these data.

### C. High-pressure transport

The increase of the  $\Gamma_6^C-\Gamma_8^V$  energy gap with hydrostatic pressure shows a quadratic dependence of the form

$$E_\Gamma = a + bP + cP^2, \quad (13)$$

where the coefficients  $a$ ,  $b$ , and  $c$  have been measured accurately by Welber *et al.*<sup>58</sup> Their values are shown in Table II. Corresponding measurements have not been made for the  $L_6^C$  and  $X_6^C$  minima, although values for other semiconductors for which these minima can be measured<sup>25</sup> show linear coefficients of the order of 0.005 and  $-0.0015$  eV/kbar for  $L_6^C$  and  $X_6^C$ , respectively.

The reinterpretation of the high-pressure transport measurements of Pitt and Lees<sup>8</sup> in terms of the three-level model proposed here presents no difficulties because the relative pressure coefficients and zero-pressure energies are such that the  $L_6^C$  minima move up sufficiently fast with increasing pressure to always lie above either  $\Gamma_6^C$  or  $X_6^C$ . By contrast to the high-temperature results,<sup>9</sup> therefore, the  $L_6^C$  minima are relatively unimportant compared to  $X_6^C$  in high-pressure work.

A comparison of the experimental<sup>8</sup> Hall coefficient and resistivity,  $\rho$ , data to that calculated theoretically within the three-minima model, using the parameters given in Tables I and II, is shown in Fig. 6. The theoretical expression for

$R_H$  is given in Eq. (5). The corresponding expression for  $\rho$  is

$$\rho = (n_\Gamma e\mu_\Gamma + n_L e\mu_L + n_X e\mu_X)^{-1}. \quad (14)$$

The theoretical curves were calculated assuming 15% carrier freezeout in  $X_6^C$ , as indicated by the asymptotic value of the Hall coefficient,<sup>8</sup> and assuming that the mobility and density of states for  $\Gamma_6^C$  varied as  $m^*^{-3/2}$  and  $m^*^{3/2}$ , respectively, in accordance with polar-optic scattering<sup>50</sup> and density-of-states theory.<sup>36</sup> The  $\mu_\Gamma$  variation produces the slow increase in  $\rho$  below 25 kbar. For  $L_6^C$  and  $X_6^C$ , the effects of changes in mobility and density of states with pressure are much smaller and were neglected.

Pitt<sup>3</sup> and Pitt and Lees<sup>8</sup> have discussed the interaction of parameters of the two-level model with respect to their measurements. The discussion applies essentially unchanged here, because as seen in Fig. 6 the  $L_6^C$  minima have no observable effect on  $\rho$  and only a minor effect on  $R_H$ . The major influence is obtained from the pressure dependence of the thresholds. Here, we have assumed the same quadratic pressure dependence for  $L_6^C$  and  $X_6^C$  on the basis that the nonlinearity arises from the effect of the  $3d$  core levels on the  $\Gamma_8^V$  (reference) valence band,<sup>58</sup> although at these relatively low pressures the effect of the quadratic term can be reproduced by simply adding  $-0.0012$  eV/kbar to the linear terms. If the  $L_6^C$  and  $X_6^C$  quadratic terms were set equal to zero, then the best-fit linear pressure coefficients for  $L_6^C$  and  $X_6^C$  in Table II would become  $+0.0043$  and  $-0.0027$  eV/bar, respectively. Although somewhat lower than the accepted values,<sup>25</sup> there exists evidence<sup>3,59</sup> that the  $X_6^C$  coefficient should be slightly more negative than the accepted value. The effect of dropping the quadratic terms for  $L_6^C$  and  $X_6^C$  while retaining the best-fit linear coefficients is also shown in Fig. 6.

The  $L_6^C$  minima, nevertheless, influence the rising part of  $R_H$  sufficiently so that the best fit can only be obtained with a lower limit of approximately  $900 \text{ cm}^2 \text{ V}^{-1} \text{ sec}^{-1}$  for the  $L_6^C$  mobility. Since the high-temperature results indicated a 8:1 minimum  $\mu_\Gamma:\mu_L$  mobility ratio, the two experiments taken together produce a reasonably definite value for  $\mu_L$ . It is interesting to note that the ratio in Table II is almost exactly that (7.5:1) determined for GaSb.<sup>57</sup> The presence of  $L_6^C$  also requires that the mobility for  $X_6^C$  be about 10% less than that obtained<sup>8</sup> from the  $\Gamma$ - $X$  model.

In a similar experiment, Harris *et al.*<sup>60</sup> measured the behavior of the threshold and the resistivity of GaAs Gunn oscillators under uniaxial stress. They found essentially no change of resistance with uniaxial stress along  $\langle 111 \rangle$  up to

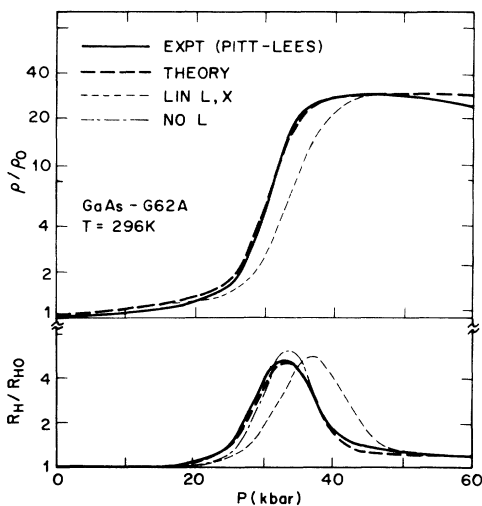


FIG. 6. Variation of resistivity and Hall coefficient with hydrostatic pressure from high-pressure transport measurements (after Ref. 8) and from various calculations within the  $\Gamma$ - $L$ - $X$  model (see text).

18 kbar, but a dramatic increase in resistance for [100] stress beginning at 8 kbar. They interpreted these results as evidence that the first indirect minima were located at  $X_6^C$ , not  $L_6^C$ .

However, the interpretation depends upon the relative magnitude of the shear deformation potentials of the  $L_6^C$  and  $X_6^C$  minima, together with contributions from the hydrostatic term. In general, the strain-induced shift of the  $i$ th minima is given by<sup>61</sup>

$$\Delta E_i = \hat{n}_i \cdot \{ (\mathcal{E}_1 \text{Tr } \underline{e}) \underline{1} + \mathcal{E}_2 [\underline{e} - (\frac{1}{3} \text{Tr } \underline{e}) \underline{1}] \} \cdot \hat{n}_i, \quad (15)$$

where  $\mathcal{E}_1$  and  $\mathcal{E}_2$  are the hydrostatic and shear deformation potentials, respectively,  $\underline{e}$  is the strain tensor, and  $\hat{n}_i$  is the unit vector of the minimum in the Brillouin zone. Only the hydrostatic term contributes for  $\Gamma_6^C$ .

The hydrostatic terms for energy shifts of  $\Gamma_6^C$ ,  $L_6^C$ , and  $X_6^C$  relative to  $\Gamma_8^V$  for a uniaxial stress can be obtained directly from Table II since they are just  $\frac{1}{3}$  the corresponding values given in Table II for hydrostatic stress. The shear deformation potentials that contribute to energy splittings of  $X_6^C$  and  $L_6^C$  for stresses along [100] and [111], respectively, are not known for GaAs. But they can be estimated from the uniaxial stress and hydrostatic pressure<sup>62</sup> data shown in Fig. 6 of Ref. 60 by noting that the resistivity versus uniaxial stress curve closely follows that of the resistivity versus hydrostatic pressure data of Refs. 8 and 62, except that the same increase in resistance was achieved for uniaxial stress values about  $\frac{1}{3}$  those for hydrostatic pressure. Thus the shear term apparently makes a given [100] uniaxial stress about three times as effective as the same isotropic (hydrostatic) stress with respect to the  $X_6^C$  minima. Using the known compliance coefficients<sup>63</sup> for GaAs, it is straightforward to show that  $\mathcal{G}_2^X = 33$  eV. This value is surprisingly large, considering that the equivalent value in Si, obtained from absorption measurements at the indirect threshold, is 8.6 eV.<sup>64</sup> A similar calculation for  $L_6^C$ , based on the lack of anomalous resistance increase to 18 kbar, shows that  $\mathcal{G}_2^L$  should be less than 14 eV, which is reasonable in view of the Ge value of 18.7 eV (Ref. 64) for this quantity.

By using the hydrostatic data to calculate the  $X_6^C$  shear deformation potential, we have essentially eliminated the distinction between the  $\Gamma$ - $L$ - $X$  and the  $\Gamma$ - $X$  models as applied to this experiment since in both models the increase in resistance is due predominantly to carrier transfer to  $X_6^C$ . Thus instead of proving that the  $X_6^C$  minima are lower in energy than the  $L_6^C$  minima, Harris *et al.*<sup>60</sup> showed that the  $X_6^C$  shear deformation potential is apparently exceptionally large. Con-

sequently, their results do not contradict those of other experiments and are not inconsistent with the  $\Gamma$ - $L$ - $X$  model. In view of the results of Pitt and Lees<sup>8</sup> regarding carrier freezeout under hydrostatic pressure in a number of GaAs samples, it is also possible that the anomalous resistance increase arises from this mechanism and is not due to a large shear deformation potential. Further work is necessary to resolve this point.

#### IV. DISCUSSION

By defining accurate values for the  $\Gamma_6^C$ ,  $L_6^C$ , and  $X_6^C$  minima in GaAs as a function of temperature, we can calculate accurate values of the energies of these minima in  $\text{GaAs}_{1-x}\text{P}_x$  alloys with the aid of existing measurements of the  $\Gamma_6^C$  direct edge variation,<sup>65</sup> the  $X_6^C$  indirect edge variation<sup>18</sup> above the crossover composition ( $x \cong 0.45$ ), and the  $L_6^C$  indirect edge position in GaP. The latter energy has not been positively identified, but anomalous structure in core-level Schottky-barrier electroreflectance spectra for<sup>66</sup> GaP approximately 0.4 eV above the  $X_6^C$  threshold in these data suggest that the  $L_6^C$  minima occur 0.4 eV above  $X_6^C$  in GaP. Using this value and assuming a bowing parameter 90% that of  $\Gamma_6^C$ , in agreement with data<sup>67</sup> for  $\text{Ga}_{1-x}\text{Al}_x\text{Sb}$  alloys, we calculate a functional dependence on  $x$  of the  $\Gamma_6^C$ ,  $L_6^C$ , and  $X_6^C$  minima for  $\text{GaAs}_{1-x}\text{P}_x$  at 77 K of

$$E_\Gamma = [1.508 + 1.366x - 0.174x(1-x)] \text{ eV}, \quad (16a)$$

$$E_L = [1.802 + 0.930x - 0.16x(1-x)] \text{ eV}, \quad (16b)$$

$$E_X = [1.971 + 0.361x - 0.202x(1-x)] \text{ eV}. \quad (16c)$$

These variations are shown in Fig. 7, with experimental data from Ref. 18. Also shown are data for the  $N_X$  and recently identified<sup>26</sup>  $N_\Gamma$  isoelectronic trap energies. The  $L_6^C$  minima are seen to be located about 100 meV above  $\Gamma_6^C$  and  $X_6^C$  at the  $E_X$ - $E_\Gamma$  crossing.

It is qualitatively evident from Fig. 7 that the binding energy of the deep state  $N_X$ , which is associated with a deep, local Koster-Slater-type potential,<sup>27</sup> must result from an interaction of the trap potential with the conduction-band densities of states around both  $L_6^C$  and  $X_6^C$ . The first-principles calculation of the binding energy of the N isoelectronic donor is a difficult problem which has not yet been solved,<sup>27,29</sup> although it can be formulated rather simply. Following Craford and Holonyak,<sup>11</sup> we write in a one-band approximation

$$[H_0 + V(\vec{r})] \phi(\vec{r}) = E_N \phi(\vec{r}), \quad (17a)$$

$$\phi(\vec{r}) = \sum_k A(k) \Phi_c(\vec{k}, \vec{r}), \quad (17b)$$

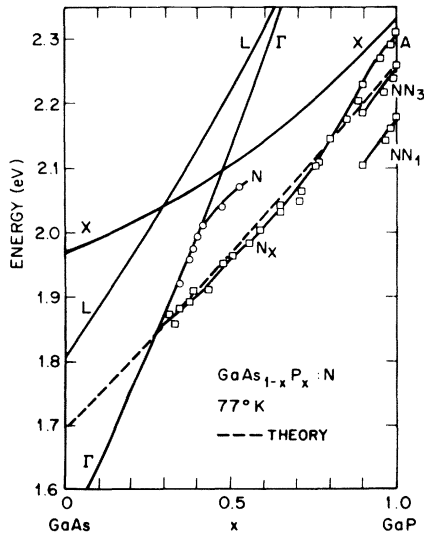


FIG. 7. Experimental (after Ref. 18) and theoretical variation of the  $\Gamma_6^c, L_6^c, X_6^c$ , nitrogen isoelectronic trap energies as a function of phosphorus fraction  $x$  in the  $\text{GaAs}_{1-x}\text{P}_x$  alloy series.

where  $H_0$  is the Hamiltonian of the unperturbed crystal,  $V(\vec{r})$  is the Koster-Slater potential,  $E_N$  and  $\phi(\vec{r})$  are the energy and wave function of an electron bound to the isoelectronic trap, and  $A(\vec{k})$  are coefficients of expansion of  $\phi(\vec{r})$  in a Bloch function basis set  $\Phi_c(\vec{k}, \vec{r})$ . Considering the large density of states of  $X_6^c$  and  $L_6^c$  relative to  $\Gamma_6^c$  and their relatively large mass, we approximate the actual Hamiltonian with a two-band model consisting of states at energies  $E_X$  and  $E_L$  with an off-diagonal interaction  $V$  between them. In this approximation we find

$$\det \begin{vmatrix} E_X - E_N & V \\ V & E_L - E_N \end{vmatrix} = 0, \quad (18)$$

in which case

$$E_N = \frac{1}{2}(E_X + E_L) - \frac{1}{2}[(E_X - E_L)^2 + 4V^2]^{1/2}, \quad (19)$$

where  $E_X$  and  $E_L$  are given by Eqs. (1).  $V$  is an adjustable parameter which may be obtained by noting that at  $E_X = E_L$ , then  $E_N = E_L - V$ . We find from Fig. 7 that  $V = 0.18$  eV. The model is somewhat oversimplified in that it neglects the increasing strain around the N isoelectronic impurity with increasing As fraction. This acts to increase  $V$  with increasing As content.<sup>68</sup> But if we assume this effect to be minor, the predicted variation of  $E_N$  with  $x$  is that shown in Fig. 7. The agreement with experiment<sup>18</sup> is remarkable, and it demonstrates conclusively the importance of the  $L_6^c$  wave-function components in the isoelectronic trap. Since the amplitude of any given wave func-

tion  $\Phi_c(\vec{k}, \vec{r})$  in  $\phi(\vec{r})$  is proportional to  $1/[E_c(\vec{k}) - E_N]$ ,<sup>11</sup> we find that the  $L_6^c$  and  $X_6^c$  components of  $\phi(\vec{r})$  should be roughly equal in amplitude at the disappearance of the bound state near  $x = 0.28$ .

Further implications of the results presented here include the following. The analysis<sup>10,31,32</sup> of transferred-electron devices of GaAs and its alloys should be reevaluated in terms of the second minima at  $L_6^c$  instead of  $X_6^c$ , with a separation energy of approximately 0.29 eV between the minima instead of 0.35 eV as is typically assumed.<sup>10</sup> No difficulties are foreseen since the increase in indirect-minima population implied by the reduction in activation energy will be compensated in part by the somewhat lower density of states mass for  $L_6^c$  (see Table II). We have also shown in Sec. III that the mobility of carriers in  $L_6^c$  is nearly an order of magnitude lower than that of carriers in  $\Gamma_6^c$  to be consistent with transport data. The rapid thermalization of hot electrons into the  $L_6^c$  minima, also required in Gunn oscillator operation, has been shown by the analysis of photoemission data by James and Moll,<sup>7</sup> which is now interpreted to involve  $L_6^c$  and not  $X_6^c$ .

Calculations<sup>11,28</sup> of the luminescence efficiency of GaAs and related semiconductor alloys will be influenced by the  $L_6^c$  components of the wave functions of the electrons on the luminescent centers, which have been neglected previously. It is clear that the normalized component involving  $\Gamma_6^c$  must decrease, and that theoretical efficiency calculations have somewhat overestimated the ultimate capability of GaAs-based devices.

Finally, we note that our value of  $170 \pm 30$  meV for the  $X_6^c - L_6^c$  energy separation is in excellent agreement with the results of recent nonlocal pseudopotential calculations, which give values of 150 (Ref. 19) and 210 meV (Ref. 20) for this quantity. These calculations had been based upon optical absorption,<sup>14</sup>  $sp^3$  valence-conduction Schottky-barrier electroreflectance,<sup>12</sup> and photoemission determinations of the width of the valence band.<sup>69</sup> One of the surprising results of the nonlocal calculation was the lowering in energy of the  $L_V^3$  symmetry point at  $-0.8$  eV in the local pseudopotential calculations by about 0.45 eV,<sup>19,20</sup> an appreciable fraction of the 1.3-eV increase in width of the entire valence band of width  $\sim 12$  eV. Together with the  $sp^3$  Schottky-barrier electroreflectance value of 3.041 eV for the  $L_6^c - L_V^3$  separation<sup>12</sup> this was sufficient to move  $L_6^c$  from 0.25 eV above to 0.2 eV below  $X_6^c$ , apparently in conflict with existing data but in excellent agreement with the results found here. This provides a further independent indication of the importance of nonlocal terms in pseudopotential and other band-structure calculations.

In summary, the  $\Gamma_6^C-L_6^C-X_6^C$  ordering of the conduction-band minima of GaAs resolves the previous discrepancies among indirect-threshold activation energies as measured by transport experiments and photoemission and intraconduction-band absorption thresholds measured optically. Secondly, the behavior of the energy of the  $L_6^C$  and  $X_6^C$  minima and that of the deep N isoelectronic trap with  $x$  in GaAs<sub>1-x</sub>P<sub>x</sub> alloys provides qualitative evidence of the importance of  $L_6^C$  components in the wave functions of electrons localized in these states. Thirdly, the  $\Gamma_6^C-L_6^C-X_6^C$  energies in Table I are in excellent agreement with the results of nonlocal pseudopotential calculations.<sup>19,20</sup> Fourthly, we predict that angle-resolved photoemission measurements should show the  $\langle 111 \rangle$  symmetry of the 1.7-eV peak in the EDC of cesiated GaAs. Finally, the modifications necessary to previous theories of operation of transferred-electron devices, light-emitting diodes, and solid-state lasers should provide the basis for greater understanding of the operation of these devices.

*Note added in proof.* Further support of the  $\Gamma-L-X$  ordering of the lower conduction-band minima of GaAs has now been obtained from velocity-field calculations,<sup>71</sup> Gunn oscillation threshold measurements under uniaxial stress,<sup>71</sup> luminescence measurements in Ga<sub>1-x</sub>Al<sub>x</sub>As alloys,<sup>72</sup>

and resonant enhancement of second-order Raman scattering spectra involving phonons at  $L$  and  $X$ .<sup>73</sup> Thus the  $\Gamma-L-X$  ordering appears to be established beyond reasonable doubt.

#### ACKNOWLEDGMENTS

It is a great pleasure to acknowledge the collaboration of C. G. Olson and D. W. Lynch and the cooperation of E. M. Rowe and the Synchrotron Radiation Center staff, with whom the core-level Schottky-barrier electroreflectance measurements were performed. I am particularly indebted to H. C. Casey for numerous useful discussions during the course of this work. Thanks are also due to N. Holonyak, Jr., for preprints of results on N-doped GaAs<sub>1-x</sub>P<sub>x</sub> alloys prior to publication, to J. A. Copeland, M. G. Craford, N. Holonyak, Jr., A. Onton, and B. Welber concerning their experimental results, and to D. J. Wolford and B. G. Streetman concerning details of the behavior of the N isoelectronic trap in GaAs<sub>1-x</sub>P<sub>x</sub> alloys. The Synchrotron Radiation Center of the Physical Sciences Laboratory of the University of Wisconsin was supported by the National Science Foundation under Grant No. DMR-74-15089. A report of this work was presented at the 1976 Device Research Conference.<sup>70</sup>

<sup>1</sup>D. E. Aspnes, C. G. Olson, and D. W. Lynch, *Phys. Rev. Lett.* **37**, 766 (1976).

<sup>2</sup>H. Ehrenreich, *Phys. Rev.* **120**, 1951 (1960).

<sup>3</sup>G. D. Pitt, *J. Phys. C* **6**, 1586 (1973).

<sup>4</sup>I. Balslev, *Phys. Rev.* **173**, 762 (1968).

<sup>5</sup>A. Onton, R. J. Chicotka, and Y. Yacoby, in *Proceedings of the 11th International Conference on the Physics of Semiconductors, Warsaw* (PWN-Polish Scientific, Warszawa, 1972), p. 1023.

<sup>6</sup>L. W. James, R. C. Eden, J. L. Moll, and W. E. Spicer, *Phys. Rev.* **174**, 909 (1968).

<sup>7</sup>L. W. James and J. L. Moll, *Phys. Rev.* **183**, 740 (1969).

<sup>8</sup>G. D. Pitt and J. Lees, *Phys. Rev. B* **2**, 4144 (1970).

<sup>9</sup>P. Blood, *Phys. Rev. B* **6**, 2257 (1972).

<sup>10</sup>J. A. Copeland and S. Knight, in *Semiconductors and Semimetals*, edited by R. K. Willardson and A. C. Beer (Academic, New York, 1971), Vol. 7, p. 3.

<sup>11</sup>M. G. Craford and N. Holonyak, Jr., in *Optical Properties of Solids: New Developments*, edited by B. O. Seraphin (North-Holland, Amsterdam, 1976), p. 187.

<sup>12</sup>D. E. Aspnes and A. A. Studna, *Phys. Rev. B* **7**, 4605 (1973).

<sup>13</sup>D. D. Sell, H. C. Casey, Jr., and K. W. Wecht, *J. Appl. Phys.* **45**, 2650 (1974).

<sup>14</sup>D. D. Sell, S. E. Stokowski, R. Dingle, and J. V. DiLorenzo, *Phys. Rev. B* **7**, 4568 (1973).

<sup>15</sup>M. B. Panish and H. C. Casey, Jr., *J. Appl. Phys.* **40**, 163 (1969).

<sup>16</sup>M. G. Craford, R. W. Shaw, A. H. Herzog, and W. O. Groves, *J. Appl. Phys.* **43**, 4075 (1972).

<sup>17</sup>W. O. Groves, A. H. Herzog, and M. G. Craford, *Appl. Phys. Lett.* **19**, 184 (1971).

<sup>18</sup>R. J. Nelson, N. Holonyak, Jr., J. J. Coleman, D. Lazarus, W. O. Groves, D. L. Keune, M. G. Craford, D. J. Wolford, and B. G. Streetman, *Phys. Rev. B* **14**, 685 (1976).

<sup>19</sup>K. C. Pandey and J. C. Phillips, *Phys. Rev. B* **9**, 1552 (1974).

<sup>20</sup>J. R. Chelikowsky and M. L. Cohen, *Phys. Rev. Lett.* **32**, 674 (1974); *Phys. Rev. B* **14**, 556 (1976).

<sup>21</sup>H. Ehrenreich, *J. Appl. Phys.* **32**, 2155 (1961).

<sup>22</sup>M. Cardona and D. L. Greenway, *Phys. Rev.* **125**, 1291 (1962).

<sup>23</sup>D. Auvergne, J. Camassel, H. Mathieu, and M. Cardona, *Phys. Rev. B* **9**, 5168 (1974).

<sup>24</sup>J. Camassel and D. Auvergne, *Phys. Rev. B* **12**, 3258 (1975).

<sup>25</sup>D. L. Camphausen, G. A. N. Connell, and W. Paul, *Phys. Rev. Lett.* **26**, 184 (1971).

<sup>26</sup>D. J. Wolford, B. G. Streetman, W. Y. Hsu, J. D. Dow, R. J. Nelson, and N. Holonyak, Jr., *Phys. Rev. Lett.* **36**, 1400 (1976).

- <sup>27</sup>R. A. Faulkner, *Phys. Rev.* **175**, 991 (1969).
- <sup>28</sup>J. C. Campbell, N. Holonyak, Jr., M. G. Craford, and D. L. Keune, *J. Appl. Phys.* **45**, 4543 (1974).
- <sup>29</sup>S. F. Ross and M. Jaros, *Solid State Commun.* **13**, 1751 (1973).
- <sup>30</sup>J. B. Gunn, *IBM J. Res. Dev.* **8**, 141 (1964).
- <sup>31</sup>B. K. Ridley and T. B. Watkins, *Proc. Phys. Soc. Lond.* **78**, 293 (1961); B. K. Ridley, *ibid.* **82**, 954 (1963).
- <sup>32</sup>C. Hilsum, *Proc. IRE* **50**, 185 (1962).
- <sup>33</sup>C. D. Thurmond, *J. Electrochem. Soc.* **122**, 1133 (1975).
- <sup>34</sup>Y. P. Varshni, *Physica (Utr.)* **39**, 149 (1967).
- <sup>35</sup>A value of  $0.467 \pm 0.005$  eV attributed to Onton is commonly found in the literature (see, e.g., Refs. 3 and 16); this represents a preliminary value that was different from the final value reported in Ref. 5 (Onton, private communication).
- <sup>36</sup>R. A. Smith, *Semiconductors* (Cambridge U.P., Cambridge, England, 1961).
- <sup>37</sup>J. G. Gay, *Phys. Rev. B* **4**, 2567 (1971).
- <sup>38</sup>G. Dolling and J. L. T. Waugh, in *Proceedings of the International Conference on Lattice Dynamics, Copenhagen*, edited by R. F. Wallis (Pergamon, London, 1965), p. 19.
- <sup>39</sup>C. J. Hwang, *J. Appl. Phys.* **40**, 3731 (1969).
- <sup>40</sup>C. D. Thurmond (private communication).
- <sup>41</sup>P. J. Dean, G. Kaminsky, and R. B. Zetterstrom, *J. Appl. Phys.* **38**, 3551 (1967).
- <sup>42</sup>A. G. Thompson, J. C. Woolley, and M. Rubenstein, *Can. J. Phys.* **44**, 2927 (1966).
- <sup>43</sup>L. W. Aukerman and R. K. Willardson, *J. Appl. Phys.* **31**, 939 (1960).
- <sup>44</sup>G. D. Pitt, *Solid State Commun.* **8**, 1119 (1970).
- <sup>45</sup>Q. H. F. Vrethen, *J. Phys. Chem. Solids* **29**, 129 (1968).
- <sup>46</sup>G. Dresselhaus and M. S. Dresselhaus, *Phys. Rev.* **160**, 649 (1967).
- <sup>47</sup>A. Onton, *Phys. Rev.* **186**, 786 (1969).
- <sup>48</sup>C. Hilsum, in *Semiconductors and Semimetals*, edited by R. K. Willardson and A. C. Beer (Academic, New York, 1966), Vol. I, p. 3.
- <sup>49</sup>D. L. Rode, *Phys. Rev. B* **2**, 1012 (1970).
- <sup>50</sup>D. L. Rode and S. Knight, *Phys. Rev. B* **3**, 2534 (1971).
- <sup>51</sup>C. Hilsum and J. Welborn, *J. Phys. Soc. Jpn. Suppl.* **21**, 532 (1966).
- <sup>52</sup>W. Fawcett, A. D. Boardman, and S. Swain, *J. Phys. Chem. Solids* **31**, 1963 (1970).
- <sup>53</sup>C. Herring, *Bell. Syst. Tech. J.* **34**, 237 (1955).
- <sup>54</sup>M. G. Craford, W. O. Groves, A. H. Herzog, and D. E. Hill, *J. Appl. Phys.* **42**, 2751 (1971).
- <sup>55</sup>H. G. B. Hicks and D. F. Manley, *Solid State Commun.* **7**, 1463 (1969).
- <sup>56</sup>A. Sagar, *Phys. Rev.* **117**, 93 (1960).
- <sup>57</sup>B. B. Kosicki, A. Jayaraman, and W. Paul, *Phys. Rev.* **172**, 764 (1968).
- <sup>58</sup>B. Welber, M. Cardona, C. K. Kim, and S. Rodriguez, *Phys. Rev. B* **12**, 5729 (1975).
- <sup>59</sup>M. Konczykowski, J. Chroboczek, and S. Porowski, in Ref. 5, p. 1050.
- <sup>60</sup>J. S. Harris, J. L. Moll, and G. L. Pearson, *Phys. Rev. B* **1**, 1660 (1970).
- <sup>61</sup>M. Cardona, *Modulation Spectroscopy* (Academic, New York, 1969).
- <sup>62</sup>A. R. Hutson, A. Jayaraman, and A. S. Coriell, *Phys. Rev.* **155**, 786 (1967).
- <sup>63</sup> $S_{11}=12.64$ ,  $S_{12}=-4.234$ , and  $S_{14}=18.6$  (units are  $10^{-13}$  cm<sup>2</sup>/dyn). See H. B. Huntington, in *Solid State Physics*, edited by F. Seitz and D. Turnbull (Academic, New York, 1958), Vol. 7, p. 213.
- <sup>64</sup>I. Balslev, *Phys. Rev.* **143**, 636 (1966).
- <sup>65</sup>R. J. Nelson, N. Holonyak, Jr., and W. O. Groves, *Phys. Rev. B* **13**, 5415 (1976).
- <sup>66</sup>D. E. Aspnes, C. G. Olson, and D. W. Lynch, *Phys. Rev. B* **14**, 2534 (1976).
- <sup>67</sup>K. Y. Cheng, G. L. Pearson, R. S. Bauer, and D. J. Chadi, *Bull. Am. Phys. Soc.* **21**, 365 (1976).
- <sup>68</sup>D. J. Wolford and B. G. Streetman (private communication and unpublished).
- <sup>69</sup>L. Ley, R. A. Pollak, F. R. McFeely, S. P. Kowalczyk, and D. A. Shirley, *Phys. Rev. B* **9**, 600 (1974).
- <sup>70</sup>D. E. Aspnes, *IEEE Trans. Electron Devices* (in press).
- <sup>71</sup>P. J. Vinson, C. Pickering, A. R. Adams, W. Fawcett, and G. D. Pitt, in *Proceedings of the 13th International Conference on the Physics of Semiconductors, Rome* (to be published).
- <sup>72</sup>R. Dingle, R. A. Logan, and J. R. Arthur, Jr., in *International Conference on GaAs and Related Materials* (to be published).
- <sup>73</sup>R. Trommer and M. Cardona, *Solid State Commun.* (to be published).